

## **Comparative study of inhibition at multiple stages of amyloid- $\beta$ self-assembly provides mechanistic insight**

Timothy J. Davis<sup>1</sup>, Deborah D. Soto-Ortega, Joseph A. Kotarek,  
Francisco J. Gonzalez-Velasquez, Krishnamoorthy Sivakumar,  
Laying Wu, Qian Wang, and Melissa A. Moss

Department of Chemical Engineering, University of South Carolina,  
Columbia, South Carolina, 29208 (T.J.D., D.D.S-O., J.A.K., F.J.G-V., M.A.M.)

Department of Chemistry and Biochemistry, University of South Carolina,  
Columbia, South Carolina, 29208 (K.S., L.W., Q.W.)

**Running Title:** Mechanistic insight into inhibition of A $\beta$  self-assembly

Address correspondence to:

Melissa A. Moss, PhD  
Department of Chemical Engineering  
University of South Carolina  
2C02 Swearingen Engineering Center  
Columbia, SC 29208  
Telephone: 803-777-5604  
Fax: 803-777-0973  
Email: [mossme@cec.sc.edu](mailto:mossme@cec.sc.edu)

**Number of text pages (including abstract, excluding references):** 25

**Number of tables:** 0

**Number of reaction schemes:** 1

**Number of figures:** 6

**Number of references:** 40

**Number of words:**

<b>Abstract</b>	243
<b>Introduction</b>	688
<b>Discussion</b>	1499

**ABBREVIATIONS:** A $\beta$ , amyloid- $\beta$  protein; AD, Alzheimer's disease; ANOVA, analysis of variance; DLS, dynamic light scattering; DMF, dimethylformamide; DMSO, dimethylsulfoxide; HFIP, hexafluoroisopropanol;  $R_H$ , hydrodynamic radius; TEM, transmission electron microscopy; ThT, thioflavin T; SEC, size exclusion chromatography.

## Abstract

The ‘amyloid cascade hypothesis’, linking self-assembly of the amyloid- $\beta$  protein ( $A\beta$ ) to the pathogenesis of Alzheimer’s disease (AD), has led to the emergence of inhibition of  $A\beta$  self-assembly as a prime therapeutic strategy for this currently unpreventable and devastating disease. The complexity of  $A\beta$  self-assembly, which involves multiple reaction intermediates related by nonlinear and interconnected nucleation and growth mechanisms, provides multiple points for inhibitor intervention. While a number of small molecule inhibitors of  $A\beta$  self-assembly have been identified, little insight has been garnered concerning the point at which these inhibitors intervene within the  $A\beta$  assembly process. In the current study, a julolidine derivative is identified as an inhibitor of  $A\beta$  self-assembly. To gain insight into the mechanistic action of this inhibitor, the inhibition of fibril formation from monomeric protein is assessed quantitatively and compared to the inhibition of two distinct mechanisms of growth for soluble  $A\beta$  aggregation intermediates. This compound is observed to significantly inhibit soluble aggregate growth by lateral association, while having little effect on soluble aggregate elongation via monomer addition. In addition, inhibition of soluble  $A\beta$  aggregate association exhibits an  $IC_{50}$  with a somewhat lower stoichiometric ratio than the  $IC_{50}$  determined for inhibition of fibril formation from monomeric  $A\beta$ . This quantitative comparison of inhibition within multiple  $A\beta$  self-assembly assays suggests that this compound binds the lateral surface of on-pathway intermediates exhibiting a range of sizes to prevent their association with other aggregates, which is required for further assembly into mature fibrils.

Alzheimer's disease (AD) is currently the most common type of dementia, affecting an estimated 5.2 million Americans (Alzheimer's Association, 2008). As the life expectancy in the United States and other post industrialized nations increases, AD presents a burgeoning epidemic. AD initially affects short-term memory and progresses to include pervasive cognitive and emotional dysfunction. These manifested symptoms are hypothesized to result from a cascade of events initiated by self-assembly of monomeric amyloid- $\beta$  protein ( $A\beta$ ), leading first to the formation of soluble aggregates and later progressing into larger insoluble fibrils which ultimately deposit in the extracellular space of the brain parenchyma. This 'amyloid cascade hypothesis' is supported by experimental evidence (reviewed in Walsh and Selkoe, 2007), including genetic correlations, transgenic animal models, and cell culture studies, and has established inhibition of  $A\beta$  self-assembly as a prime therapeutic strategy in the fight against AD.

Several small molecules that inhibit the *in vitro* formation of amyloid fibrils from monomeric  $A\beta$  have been identified (reviewed in Findeis, 2000; Hamaguchi et al., 2006; LeVine, 2007). Studies employing quantitative measures of inhibition assembled from light scattering measurements, thioflavin T (ThT) fluorescence, or immunoassays have facilitated comparisons of inhibitory potential among different molecular structures (e.g., Byeon et al., 2007; Dolphin et al., 2008; Ferrao-Gonzales et al., 2005; Howlett et al., 1999a; Howlett et al., 1999b; Ono et al., 2004; Ono et al., 2003; Reinke and Gestwicki, 2007; Simons et al., 2009). The majority of these studies, however, have quantified the effect of small molecule inhibitors on the overall extent of fibril formation, without recognition that  $A\beta$  self-assembly is a complex process involving multiple pathways and numerous on-pathway assembly intermediates, including oligomers, protofibrils, and other soluble aggregates (LeVine, 2007; Necula et al., 2007b). Some small

molecule inhibitors selectively halt the formation of mature A $\beta$  fibrils from monomer without stopping the formation of soluble aggregates (Bohrmann et al., 2000) or the growth of pre-formed fibrils (LeVine, 2007). Alternatively, small molecule inhibitors have been observed to promote fibril formation but inhibit ongoing fibril growth (Williams et al., 2005) and to selectively inhibit different mechanisms of soluble aggregate growth (Moss et al., 2004). In addition, while some small molecules prevent both oligomer and fibril formation (Bastianetto et al., 2006; De Felice et al., 2004; Howlett et al., 1999a; Necula et al., 2007b; Yang et al., 2005), other inhibitors halt the appearance of oligomers without altering mature fibril formation (Necula et al., 2007a) or, conversely, block the appearance of mature fibrils while permitting oligomer formation (Ferrao-Gonzales et al., 2005; Lashuel et al., 2002; Necula et al., 2007b). These qualitative studies demonstrate that small molecule inhibitors of A $\beta$  self-assembly can selectively act upon various assembly pathways.

Quantitative measures can provide additional information about inhibitor action but have been infrequently used to assess the ability of a single compound to interrupt different steps along the self-assembly pathway. Some small molecules have been shown to inhibit the distinct processes of fibril formation and fibril extension with similar IC<sub>50</sub> values (Dolphin et al., 2008; Ono et al., 2004; Ono et al., 2003). However, these studies examined mature A $\beta$  fibrils, which are end products of the assembly process, but did not consider soluble A $\beta$  aggregates, currently speculated to play a principal role in AD progression (reviewed in Kirkitadze et al., 2002; Walsh and Selkoe, 2007). In the current study, a julolidine aldehyde is investigated quantitatively for its ability to prevent A $\beta$ <sub>1-40</sub> fibril formation from monomer and to slow the growth of soluble A $\beta$ <sub>1-40</sub> aggregates via two distinct mechanisms, elongation by monomer addition and direct lateral association (Nichols et al., 2002). While soluble aggregate elongation is unaffected,

inhibition of both the extent of aggregate formation from monomeric protein and the growth of soluble aggregates by lateral association is observed, suggesting interaction with an on-pathway intermediate and indicating the contribution of lateral aggregate association to final aggregate content.  $IC_{50}$  values determined for these two processes suggest that this inhibitor is capable of binding a range of aggregate sizes, including aggregate species that appear early in the self-assembly pathway. Together, these results illustrate the mechanistic insight provided by quantitative comparisons of inhibitor action at different stages of A $\beta$  self-assembly.

## Materials and Methods

### Materials

A $\beta$ <sub>1-40</sub> peptide was purchased from AnaSpec (San Jose, CA) or W.M. Keck Biotechnology Resource Laboratory at Yale University (New Haven, CT). Hexafluoroisopropanol (HFIP), ThT, phosphorous oxychloride, 8-hydroxyjulolidine, dimethylformamide (DMF), and sodium bicarbonate were obtained from Sigma (St. Louis, MO). Bovine serum albumin and dimethylsulfoxide (DMSO) were obtained from EMD Chemicals (Gibbstown, NJ). Uranyl acetate was obtained from Electron Microscopy Sciences (Hatfield, PA).

### Preparation of A $\beta$ <sub>1-40</sub> Monomer and Soluble Aggregates

Lyophilized A $\beta$ <sub>1-40</sub> peptide was stored desiccated at -20°C until reconstitution and preparation as described previously (Gonzalez-Velasquez and Moss, 2008; Kotarek et al., 2008). Briefly, A $\beta$ <sub>1-40</sub> peptide was reconstituted in 50 mM NaOH at a concentration of 2 mg/ml, and pre-existing aggregates were removed by size exclusion chromatography (SEC) on a Superdex 75 HR10/30 column (GE Healthcare, Piscataway, NJ) pretreated with bovine serum albumin. A $\beta$ <sub>1-40</sub> monomer concentrations were determined from UV absorbance at 276 nm using an extinction coefficient of 1450 M<sup>-1</sup> cm<sup>-1</sup> (Nichols et al., 2002). Isolated A $\beta$ <sub>1-40</sub> monomer was used fresh or stored at 4°C for up to 48 h.

Soluble A $\beta$ <sub>1-40</sub> aggregates were prepared from isolated monomeric A $\beta$ <sub>1-40</sub> as described previously (Gonzalez-Velasquez and Moss, 2008; Kotarek et al., 2008). Briefly, monomeric A $\beta$ <sub>1-40</sub> (100-200  $\mu$ M) was agitated vigorously at 25°C for 4-15 h in the presence of 2-10 mM NaCl and 40 mM Tris-HCl (pH 8.0). Aggregation was monitored by ThT fluorescence as

described below. Soluble A $\beta_{1-40}$  aggregates were separated from fibril via centrifugation and from unreacted monomer via SEC on a Superdex 75 column. Soluble A $\beta_{1-40}$  aggregate concentrations, expressed in monomer units, were determined from UV absorbance at 276 nm corrected for light scattering (Nichols et al., 2002), and equivalent ThT measurements were determined. Isolated soluble aggregates were stored at 4°C and used for experimentation within 36 h of purification. Following storage, ThT fluorescence measurements were employed to correct for any change in aggregate concentration and dynamic light scattering (DLS) measurements were assessed to ensure that aggregates maintained their initial size.

### **Detection of A $\beta_{1-40}$ Aggregates using ThT**

The presence of amyloid aggregates was monitored via fluorescence determination as described previously (Gonzalez-Velasquez and Moss, 2008; Kotarek et al., 2008) for solutions containing A $\beta_{1-40}$  in the presence of 10  $\mu$ M or 40  $\mu$ M ThT and 40 mM Tris-HCl (pH 8.0). ThT fluorescence was measured using an LS-45 luminescence spectrometer (Perkin-Elmer, Waltham, MA) with excitation at 450 nm and excitation and emission slits of 10 nm. For HFIP-induced monomer aggregation experiments, ThT fluorescence was continuously monitored at 482 nm. For all other experiments, ThT fluorescence emission from 470 to 500 nm was measured periodically, and reported fluorescence values (F) are the integrated area under the emission curve.

### **Determination of Soluble A $\beta_{1-40}$ Aggregate Size using DLS**

As described previously (Gonzalez-Velasquez and Moss, 2008; Kotarek et al., 2008), aggregate size was assessed for undiluted samples via hydrodynamic radius ( $R_H$ ) measurements

using a DynaPro MSX DLS instrument (Wyatt Technology, Santa Barbara, CA) to assimilate auto-correlated light intensity data for calculation of translational diffusion coefficients that could be converted to  $R_H$  using the Stokes-Einstein equation. Values of  $R_H$  are reported as the intensity-weighted mean  $R_H$  (using Dynamics software by Wyatt Technology).

### **Synthesis of 8-Hydroxy-2,3,6,7-tetrahydro-1H,5H-pyrido[3,2,1-ij]quinoline-9-carbaldehyde**

8-Hydroxy-2,3,6,7-tetrahydro-1H,5H-pyrido[3,2,1-ij]quinoline-9-carbaldehyde (**2**) was identified as a promising inhibitor of A $\beta$  self-assembly following the screening of a large library of aromatic compounds (unpublished results). To synthesize this compound (Scheme 1), phosphorous oxychloride (0.11 g, 0.70 mmol) was added dropwise to a pre-cooled solution of DMF (2 ml) at 0°C, and the mixture was stirred at this temperature for 30 min. To this mixture, a solution of 8-hydroxyjulolidine (**1**) (120 mg, 0.63 mmol) in DMF (2 ml) was added dropwise in a period of 45 min at 0°C, while the color of the reaction mixture turned to green from colorless. The reaction was heated gradually to 80°C. Then, the reaction was quenched by pouring into 20 g of ice and the pH was adjusted to neutral using saturated sodium bicarbonate solution. Upon being stirred at 25°C overnight, the precipitated product was collected by filtration. Washing with water and recrystallization from hexane yielded 90 mg of a buff colored solid; yield 65%.  $^1\text{H}$  NMR (300 MHz,  $\text{CDCl}_3$ ): 9.40 (s, 1H), 6.80 (s, 1H), 3.23 (m, 4H), 2.64-2.70 (m, 4H), 1.84-1.89 (m, 4H).

### **Dissolution of Compound 2 for Experimentation**

Compound **2** was dissolved at 2-20 mM in DMSO and stored at -20°C. Stock solutions of compound **2** were diluted in DMSO such that subsequent dilution into final reactions resulted

in varying concentrations of compound **2** in the presence of a constant 2.5% (v/v) DMSO. 2.5% (v/v) DMSO was also added to control reactions run in parallel. This level of DMSO was confirmed to have no interference with DLS signals used to monitor association reactions. For association reactions, stock solutions of compound **2** were additionally filtered through a 0.2  $\mu$ m polytetrafluoroethylene Minispine Acrodisc syringe filter (Pall Life Sciences, Ann Arbor, MI) prior to dilution to ensure a clean light scattering signal. UV measurements confirmed negligible loss of the compound during the filtering procedure.

### **ThT Detection of A $\beta$ <sub>1-40</sub> Aggregates in the Presence of Compound **2****

ThT detection of A $\beta$ <sub>1-40</sub> aggregates in the presence of compound **2** was carried out to ensure that ThT fluorescence is unchanged by the simultaneous binding of both compounds to A $\beta$ <sub>1-40</sub> aggregates. Unpurified A $\beta$ <sub>1-40</sub> aggregate preparations in 40 mM Tris-HCl (pH 8.0) were combined with compound **2** and ThT. Incubations contained either 2  $\mu$ M A $\beta$ <sub>1-40</sub> aggregates, 0-50  $\mu$ M compound **2** with 2.5% (v/v) DMSO, and 10  $\mu$ M ThT to reflect expected final concentrations in monomer aggregation assay measurements or 20  $\mu$ M soluble A $\beta$ <sub>1-40</sub> aggregates, 0-500  $\mu$ M compound **2** with 2.5% (v/v) DMSO, and 40  $\mu$ M ThT to reflect expected final concentrations in HFIP-induced monomer aggregation assays. Solutions were incubated without agitation at 4°C for 15 min to ensure complete binding, and ThT fluorescence was evaluated. Detection is expressed as the percentage of the total fluorescence that was observed for an equivalent concentration of soluble A $\beta$ <sub>1-40</sub> aggregates in the absence of compound **2**.

### **A $\beta$ <sub>1-40</sub> Monomer Aggregation Assay**

SEC-isolated A $\beta$ <sub>1-40</sub> monomer in 40 mM Tris-HCl (pH 8.0) was combined with compound **2** in the presence of NaCl for final concentrations of 20  $\mu$ M monomer, 150 mM NaCl, and 0-400  $\mu$ M compound **2** with 2.5% (v/v) DMSO, where reactions containing 0  $\mu$ M compound **2** served as the positive control. Reactions were incubated at 25°C under continuous agitation (vortex, 800 rpm) to promote nucleation. During the time course of aggregation, 20  $\mu$ l aliquots were periodically withdrawn from the reaction solution, combined with 140  $\mu$ l of 10  $\mu$ M ThT, and evaluated for ThT fluorescence.

### **HFIP-induced A $\beta$ <sub>1-40</sub> Monomer Aggregation Assay**

SEC-isolated A $\beta$ <sub>1-40</sub> monomer in 40 mM Tris-HCl (pH 8.0) was combined with compound **2** in the presence of ThT and incubated at 4°C for 15 min to ensure complete binding. To initiate monomer aggregation, diluted HFIP was added for final concentrations of 2.5% (v/v) HFIP, 20  $\mu$ M A $\beta$ <sub>1-40</sub> monomer, 0-500  $\mu$ M compound **2** with 2.5% (v/v) DMSO, and 40  $\mu$ M ThT, where reactions containing 0  $\mu$ M compound **2** served as the positive control. Reactions were incubated without agitation at 25°C, and ThT fluorescence was continuously monitored. Plateau fluorescence values were taken as representative of the total aggregate formation, and aggregate formation is reported as a percentage of the positive control.

### **Soluble A $\beta$ <sub>1-40</sub> Aggregate Elongation Assay**

SEC-isolated soluble A $\beta$ <sub>1-40</sub> aggregates in 40 mM Tris-HCl (pH 8.0) were combined with compound **2** in the presence of ThT and incubated without agitation at 4°C for 15 min to allow binding. To initiate aggregate growth by elongation, SEC-isolated A $\beta$ <sub>1-40</sub> monomer was added

for final concentrations of 20  $\mu\text{M}$   $\text{A}\beta_{1-40}$  monomer, 1  $\mu\text{M}$  soluble  $\text{A}\beta_{1-40}$  aggregates, 0-80  $\mu\text{M}$  compound **2** with 2.5% (v/v) DMSO, and 10  $\mu\text{M}$  ThT. Reactions containing 0  $\mu\text{M}$  compound **2** served as the positive control. Reactions were incubated without agitation at 25°C. Incorporation of monomer into growing aggregates, or aggregate elongation, was monitored by periodically evaluating ThT fluorescence. Experiments in which ThT fluorescence of soluble  $\text{A}\beta_{1-40}$  aggregates was monitored in the absence of added monomer or the ThT fluorescence of  $\text{A}\beta_{1-40}$  monomer was monitored in the absence of added soluble aggregates served as negative controls and reflected the stability of soluble aggregates and monomer, respectively. Results are reported as the change in ThT fluorescence with time. Elongation rates were determined by regression of the linear portion of this data. The percent inhibition was calculated from the ratio of the experimental elongation rate to the elongation rate observed in the absence of inhibitor.

### **Soluble $\text{A}\beta_{1-40}$ Aggregate Association Assay**

SEC-isolated soluble  $\text{A}\beta_{1-40}$  aggregates in 40 mM Tris-HCl (pH 8.0) were combined with filtered compound **2** and incubated without agitation at 4°C for 15 min to allow binding. To initiate aggregate growth by association, concentrated NaCl was added for final concentrations of 150-300 mM NaCl, 1 or 2  $\mu\text{M}$  soluble  $\text{A}\beta_{1-40}$  aggregates, and 0-40  $\mu\text{M}$  compound **2** with 2.5% (v/v) DMSO, where reactions containing 0  $\mu\text{M}$  compound **2** served as the positive control. Concentration ranges for both soluble  $\text{A}\beta_{1-40}$  aggregates and NaCl were employed as a result of the inherent variation in association rates among soluble  $\text{A}\beta_{1-40}$  aggregate preparations. Parallel positive control and inhibition reactions performed within a single experiment were designed to contain identical concentrations of both soluble  $\text{A}\beta_{1-40}$  aggregates and NaCl. Reactions were incubated without agitation at 25°C. Association of aggregates was monitored via measurement

of increases in aggregate  $R_H$  using DLS. Experiments in which  $R_H$  of soluble  $A\beta_{1-40}$  aggregates was monitored in the absence of added NaCl served as a negative control and reflected the stability of the soluble  $A\beta_{1-40}$  aggregates. Results are reported as the change in  $R_H$  with time. Association rates were determined by regression of the linear portion of this data and are reported as a percentage of positive control. The percent inhibition was calculated from the ratio of the experimental association rate to the association rate observed in the absence of inhibitor.

### **Transmission Electron Microscopy (TEM)**

A 20  $\mu$ l sample containing soluble  $A\beta_{1-40}$  aggregates was placed upon a formvar supported Ni grid (Electron Microscopy Sciences). The sample solution was wicked away using a piece of filter paper placed at the bottom side of the grid. Sample application was repeated in this manner until the grid contained a sufficient quantity of sample for visualization. The gridded sample was then stained with 2% uranyl acetate for 12 min. The staining solution was wicked away from the grid edge, and the grid was allowed to air dry. The dried grid was visualized using a Hitachi H-8000 transmission electron microscope (Pleasanton, CA).

### **Statistical Analysis**

Statistical analysis was performed using GraphPad Prism 5 software (San Diego, CA). Differences among independent groups were assessed using a one-way analysis of variance (ANOVA), where  $p < 0.05$  was considered significant. Linear and nonlinear regressions were assessed using the coefficient of determination,  $r^2$ .

## Results

### Compound 2 Inhibits Aggregation of A $\beta$ <sub>1-40</sub> Monomer

To characterize the effect of compound **2** on the self-assembly of A $\beta$ , the 40-residue isoform of A $\beta$ , A $\beta$ <sub>1-40</sub>, was selected. A $\beta$ <sub>1-40</sub> is the most abundant isoform *in vivo* (Walsh and Selkoe, 2007) and the compositional analysis of amyloid plaques suggests that A $\beta$ <sub>1-40</sub> deposits at more advanced stages of plaque formation (Guntert et al., 2006). These characteristics render A $\beta$ <sub>1-40</sub> practical for studying later stages of A $\beta$  self-assembly that will be considered in more detail in this study. A $\beta$ <sub>1-40</sub> monomer aggregation was induced by continuous agitation in the presence of salt, and the appearance of  $\beta$ -sheet aggregates was monitored using ThT fluorescence. This assay format facilitated the rapid characterization of aggregation behavior without regard to growth mechanism. Similar aqueous-based assay formats have been used to identify other small molecule inhibitors of A $\beta$  self-assembly (e.g., Dolphin et al., 2008; Kanapathipillai et al., 2005; Ono et al., 2004; Ono et al., 2003). Extensions of the lag time, reductions in the rate of fluorescence increase, and decreases in the plateau fluorescence have all been employed as positive measures of inhibition.

Aggregation of 20  $\mu$ M A $\beta$ <sub>1-40</sub> monomer displayed a time course of ThT fluorescence characteristic of A $\beta$  self-assembly, which exhibited a lag time that was followed by a period of rapid growth and concluded with a plateau as equilibrium was reached (Fig. 1). The presence of 2.5% DMSO, employed to facilitate solubilization of compound **2**, had a negligible effect on aggregation of 20  $\mu$ M A $\beta$ <sub>1-40</sub> monomer (data not shown). When compound **2** was present at concentrations equimolar with A $\beta$ <sub>1-40</sub> monomer, the lag time was increased, indicating the inhibition of A $\beta$ <sub>1-40</sub> self-assembly by compound **2**. At a concentration 2-fold in excess of A $\beta$ <sub>1-40</sub> monomer, compound **2** additionally reduced the rate of growth observed following the lag

period, indicating a more pronounced inhibition of  $A\beta_{1-40}$  self-assembly at a higher concentration of this small molecule. When the concentration of compound **2** was further increased to a level 20-fold in excess of  $A\beta_{1-40}$  monomer, nearly complete inhibition was observed over the 1.5 h period. These results demonstrate that the presence of compound **2** results in a dose-dependent decrease in the formation of  $A\beta_{1-40}$  aggregates from monomeric protein.

### **ThT Fluorescence of Pre-formed $A\beta_{1-40}$ Aggregates is Unchanged in the Presence of Compound **2****

An alternative explanation for the data presented in Fig. 1 might be that compound **2** impedes the detection of  $A\beta$  aggregates via disruption of the binding of ThT to the amyloid  $\beta$ -sheet structure. Such a complication has been observed for other small molecules that recognize aggregated forms of  $A\beta$ , including the ThT analog BTA-1 (LeVine, 2005) and the unrelated compound nordihydroguaiaretic acid (Moss et al., 2004). To discount this possible explanation for the observed reductions in fluorescence, ThT detection of pre-formed  $A\beta_{1-40}$  aggregates was assessed in the presence of compound **2**.  $A\beta_{1-40}$  aggregates formed in the absence of compound **2** were incubated with both ThT and compound **2**, and the decrease in fluorescence detection relative to that observed for aggregates incubated with ThT alone was determined. As shown in Fig. 2, the fluorescence detection of 2  $\mu$ M  $A\beta_{1-40}$  aggregates in the presence of 10  $\mu$ M ThT was decreased by at most 15% in the presence of concentrations of compound **2** as high as 50  $\mu$ M. These concentrations are representative of the diluted samples employed for measurements in the aqueous-based  $A\beta_{1-40}$  monomer aggregation assay, where excess concentrations of compound **2** led to reductions in ThT fluorescence of 58-96%. This result confirms that reductions in fluorescence observed during  $A\beta_{1-40}$  monomer aggregation

assays are reflective of the dose-dependent inhibition of A $\beta$ <sub>1-40</sub> monomer aggregation by compound **2**, and not the disruption of A $\beta$ <sub>1-40</sub> aggregate detection by ThT.

### **Dose-Dependent Inhibition of A $\beta$ <sub>1-40</sub> Monomer Aggregation in Dilute HFIP by Compound **2** is Quantitatively Assessed**

Incubation of monomeric A $\beta$ <sub>1-40</sub> in dilute HFIP leads to the rapid formation of aggregates, which is attributed to the presence of microdroplets of HFIP within the aqueous solution. These aggregates display increased ThT fluorescence and a high content of  $\beta$ -structure characteristic of A $\beta$ <sub>1-40</sub> aggregates formed when aggregation is induced by agitation and high ionic strength (Nichols et al., 2005). However, relative to the formation of A $\beta$ <sub>1-40</sub> aggregates induced by agitation and high ionic strength, A $\beta$ <sub>1-40</sub> aggregate formation induced in the presence of dilute HFIP exhibits an abolished lag phase, during which stochastic nucleation events occur, and yields a more uniform aggregate population consisting of predominantly soluble aggregate structures (Nichols et al., 2005). In combination with a time course that is several orders of magnitude shorter, these reaction conditions result in a highly reproducible A $\beta$ <sub>1-40</sub> monomer aggregation that is more amenable to quantitative evaluation. As a result, to quantify the effect of compound **2** on the overall extent of A $\beta$ <sub>1-40</sub> self-assembly, aggregation of A $\beta$ <sub>1-40</sub> monomer was carried out in the presence of dilute HFIP and monitored *in situ* using ThT fluorescence.

When 20  $\mu$ M A $\beta$ <sub>1-40</sub> monomer was incubated in the presence of 2.5% HFIP, an immediate and rapid increase in ThT fluorescence was observed and a plateau in fluorescence was reached within 20 min (Fig. 3A). This time course for aggregate formation in the presence of dilute HFIP was similar to that observed by Nichols *et al* (2005). As for monomer aggregation induced by agitation and high ionic strength, the presence of 2.5% DMSO,

employed to facilitate solubilization of compound **2**, had a negligible effect on aggregation of 20  $\mu\text{M}$   $\text{A}\beta_{1-40}$  monomer in dilute HFIP (data not shown). When  $\text{A}\beta_{1-40}$  monomer was pre-incubated with compound **2** prior to addition of HFIP, a decrease in both the rate of increase in ThT fluorescence and the plateau fluorescence level were observed (Fig. 3A), indicative of the ability of compound **2** to inhibit, respectively, the rate at which monomeric  $\text{A}\beta_{1-40}$  is converted into  $\beta$ -sheet aggregates and the overall extent of aggregate formation. Again, insignificant changes in ThT detection of pre-formed  $\text{A}\beta_{1-40}$  aggregates were noted under these assay conditions (Fig. 2, 20  $\mu\text{M}$   $\text{A}\beta_{1-40}$ ), confirming that the observed reductions in fluorescence are indicative of inhibition. Reduction in fluorescence became more pronounced as the concentration of compound **2** was increased from 60  $\mu\text{M}$  to 200  $\mu\text{M}$ , illustrating the dose-dependence of the inhibition. The ability of compound **2** to dose-dependently reduce  $\text{A}\beta_{1-40}$  aggregate formation was quantitatively assessed via comparison of experimental plateau ThT fluorescence values to those of the control (Fig. 3B). Using 10 different stoichiometric ratios of compound **2** to  $\text{A}\beta_{1-40}$  monomer, each employing an  $\text{A}\beta_{1-40}$  monomer concentration of 20  $\mu\text{M}$ , an  $\text{IC}_{50}$  value of 6.8 was determined, indicating that a nearly 7-fold excess of compound **2** is required to observe 50% inhibition of  $\text{A}\beta_{1-40}$  aggregate formation from monomeric protein.

### **Compound 2 Fails to Alter Soluble $\text{A}\beta_{1-40}$ Aggregate Elongation via Monomer Addition**

Assays that examine the extent of aggregate formation from monomeric protein are effective at identifying inhibitors and assessing their relative efficacy. However, mechanistic specific assays are needed to ascertain the effect of an inhibitor on specific stages of aggregate growth that occur along the assembly pathway between monomer and mature fibril. In one known growth mechanism, existing  $\text{A}\beta_{1-40}$  aggregates grow via addition of monomeric protein.

This growth process creates new amyloid material, increases aggregate size, and results in aggregates with a mass per unit length similar to the starting material, suggesting that monomeric units are incorporated at the ends of growing aggregates (Nichols et al., 2002). The growth of soluble  $A\beta_{1-40}$  aggregates via addition of monomer was resolved by incubation of isolated soluble aggregates in low ionic strength buffer and in the presence of excess monomeric protein. The incorporation of monomer into growing aggregates was monitored as the change in ThT fluorescence.

As shown in Fig. 4, while  $A\beta_{1-40}$  monomer or soluble aggregates incubated alone exhibited negligible changes in aggregate content, a steady increase in aggregate content was observed when 1  $\mu\text{M}$  soluble  $A\beta_{1-40}$  aggregates were incubated in the presence of 20  $\mu\text{M}$   $A\beta_{1-40}$  monomer. Again, the presence of 2.5% DMSO had a negligible effect on the growth of 1  $\mu\text{M}$  soluble  $A\beta_{1-40}$  aggregates initiated by addition of 20  $\mu\text{M}$  monomer (data not shown). When soluble  $A\beta_{1-40}$  aggregates were incubated with equimolar concentrations of compound **2** prior to addition of  $A\beta_{1-40}$  monomer to stimulate aggregate growth, the rate of aggregate growth was similar to that observed when soluble aggregates and monomer were incubated alone, indicating no inhibition. The absence of inhibition persisted as the concentration of compound **2** was raised to 5-fold in excess of soluble  $A\beta_{1-40}$  aggregate. At significantly higher concentrations of compound **2** that exceeded both soluble  $A\beta_{1-40}$  aggregate and  $A\beta_{1-40}$  monomer, only a slight decrease in the rate of aggregate growth was noted. At the highest concentration of compound **2**, inhibition did not exceed 10%.

Results from ThT measurements were supported by TEM images acquired following 30 min of aggregate growth by elongation. 2  $\mu\text{M}$  soluble  $A\beta_{1-40}$  aggregates elongated via addition of 20  $\mu\text{M}$   $A\beta_{1-40}$  monomer (Fig. 5B) exhibited filament lengths significantly longer than soluble

aggregates incubated alone (Fig. 5A,D). When 2  $\mu\text{M}$  soluble  $\text{A}\beta_{1-40}$  aggregates were pre-incubated and elongated in the presence of 60  $\mu\text{M}$  compound **2**, a similar lengthening of filaments occurred (Fig. 5C), further illustrating the inability of this compound to halt aggregate growth via monomer addition. Together, these results illustrate that compound **2** displays insignificant inhibition of soluble  $\text{A}\beta_{1-40}$  aggregate elongation.

### **Compound 2 Inhibits the Association of Soluble $\text{A}\beta_{1-40}$ Aggregates in a Dose-Dependent Manner**

Another distinct mechanism of soluble  $\text{A}\beta_{1-40}$  aggregate growth is that of aggregate association, in which aggregates increase in size in the absence of monomeric protein via direct aggregate-aggregate interactions. This growth process leads to an increase in aggregate size in the absence of an increase in amyloid material, and the resulting aggregates exhibit a mass per unit length larger than the starting material, suggesting that association occurs in a lateral fashion (Nichols et al., 2002). The growth of soluble  $\text{A}\beta_{1-40}$  aggregates by association was resolved by incubation of isolated soluble aggregates in the absence of monomeric protein and in the presence of high ionic strength buffer. Here, because new  $\beta$ -sheet amyloid material was not formed, aggregate growth was instead monitored by measuring changes in  $R_H$  via DLS.

As shown in Fig. 6A, while soluble  $\text{A}\beta_{1-40}$  aggregates incubated in low ionic strength buffer alone exhibited negligible changes in  $R_H$ , a steady increase in  $R_H$  was observed when 2  $\mu\text{M}$  soluble  $\text{A}\beta_{1-40}$  aggregates were incubated in the presence of 260 mM NaCl. The presence of 2.5% DMSO had a negligible effect on growth of 1  $\mu\text{M}$  or 2  $\mu\text{M}$  soluble  $\text{A}\beta_{1-40}$  aggregates by association (data not shown). When soluble  $\text{A}\beta_{1-40}$  aggregates were incubated with equimolar concentrations of compound **2** prior to addition of NaCl to stimulate aggregate association, the

observed association rate, or rate of increase in  $R_H$ , was reduced by 55%, indicating a significant inhibition of aggregate association. At concentrations of compound **2** 2.15-fold in excess of soluble  $A\beta_{1-40}$  aggregates, a more pronounced 82% inhibition was evidenced, indicating the dose-dependence of compound **2** inhibition of soluble aggregate association.

The inhibitory capabilities of compound **2** for soluble aggregate association were confirmed using TEM images acquired 30 min after the initiation of aggregate growth by association. 2  $\mu$ M soluble  $A\beta_{1-40}$  aggregates incubated in low ionic strength buffer existed as short individual single stranded filaments (Fig. 5A,D), while an equivalent concentration of soluble  $A\beta_{1-40}$  aggregates incubated in the presence of elevated ionic strength exhibited clusters in which two or more filaments were bundled together (Fig. 5E). The staggered alignment of individual filaments led to the appearance of a network of longer, thicker fibrils. In contrast, when 2  $\mu$ M soluble  $A\beta_{1-40}$  aggregates were pre-incubated and associated in the presence of 40  $\mu$ M compound **2**, many individual filaments remained (Fig. 5F), illustrating inhibition of soluble aggregate association. Inhibition was not complete, however, as some grouped filaments were still observed in the presence of compound **2**.

The ability of compound **2** to dose-dependently inhibit the rate of association of soluble  $A\beta_{1-40}$  aggregates was quantitatively assessed via comparison of the experimental association rate with that observed for the control (Fig. 6B). Using 7 different stoichiometric ratios of compound **2** to soluble  $A\beta_{1-40}$  aggregates, which employed  $A\beta_{1-40}$  aggregate concentrations of either 1  $\mu$ M or 2  $\mu$ M, an  $IC_{50}$  value of 0.92 was determined, indicating that approximately equimolar quantities of compound **2** are required to observe 50% inhibition of the growth of soluble  $A\beta_{1-40}$  aggregates via association. Furthermore,  $IC_{50}$  fits revealed a maximal inhibition

of 90%, in agreement with the incomplete inhibition observed using TEM for soluble aggregate association in the presence of excess amounts of compound **2**.

## Discussion

Numerous small molecules have been identified as inhibitors of A $\beta$  self-assembly (reviewed in De Felice and Ferreira, 2002; Findeis, 2000; Hamaguchi et al., 2006; Porat et al., 2006). However, elucidation of the mechanism of inhibitor action has proven challenging as a result of the complex nature of the A $\beta$  self-assembly process. Progression from monomeric protein to the mature fibril that deposits in AD brain involves multiple reaction intermediates related by nonlinear and interconnected nucleation and growth mechanisms (LeVine, 2007; Necula et al., 2007b). When inhibition measurements consider only fibrillar end products of the self-assembly process, little information is gained concerning the point of inhibitor intervention within this nonlinear pathway. To provide mechanistic insight into inhibition of A $\beta$ <sub>1-40</sub> assembly, we have employed multiple assay formats to quantitatively assess the ability of a julolidine aldehyde to prevent the formation of aggregates from monomeric protein and to attenuate the growth of soluble aggregation intermediates via both monomer addition and aggregate association.

The inhibitory capability of this compound was first assessed using an aqueous-based A $\beta$ <sub>1-40</sub> monomer aggregation assay monitored via ThT fluorescence. The observed extension of the lag time and reduction in the rate of fluorescence increase (Fig. 1) were taken as evidence that compound **2** inhibits the formation of aggregates from monomeric A $\beta$ <sub>1-40</sub>. Unfortunately, the long time course and inherent variability of stochastic nucleation render this assay more effective for qualitatively identifying inhibition than in providing reproducible, quantitative information about the dose-dependence of inhibitor action. Thus, the more reproducible aggregation of A $\beta$ <sub>1-40</sub> monomer induced in the presence of HFIP (Nichols et al., 2005) was employed to quantitatively examine the dose-dependent inhibition of aggregate formation by

compound **2**. HFIP-induced aggregation of A $\beta$ <sub>1-40</sub> monomer has been used to quantify inhibitory activity of well known A $\beta$  aggregation inhibitors, and IC<sub>50</sub> values determined using the maximum ThT fluorescence as a measure of inhibition were in close agreement with IC<sub>50</sub> values established using aqueous-based assays (Cellamare et al., 2008). Using this approach, an IC<sub>50</sub> at a stoichiometric ratio of 6.8 compound **2** to A $\beta$ <sub>1-40</sub> was ascertained (Fig. 3B). This IC<sub>50</sub> value, which is reflective of a combination of binding affinity and stoichiometry, might suggest that compound **2** acts by binding A $\beta$ <sub>1-40</sub> monomers to prevent nucleation, as has been suggested for the inhibition of A $\beta$ <sub>1-40</sub> monomer aggregation by daunomycin (Howlett et al., 1999a) and the inhibition of A $\beta$ <sub>1-42</sub> monomer aggregation by rifamycin and hematin (Necula et al., 2007b). Alternatively, compound **2** may bind on-pathway aggregates to prevent their progression into mature fibrillar structures. This mechanism of inhibition has been inferred from the observed inhibition of A $\beta$ <sub>1-40</sub> fibril formation by benzofurans which are incapable of binding monomeric protein (Howlett et al., 1999b) as well as the ability of bis-ANS (Ferrao-Gonzales et al., 2005) and catecholamines (Lashuel et al., 2002) to prevent, respectively, the formation of A $\beta$ <sub>1-42</sub> and A $\beta$ <sub>1-40</sub> fibrils without halting the appearance of oligomeric structures.

The possibility that compound **2** may bind on-pathway intermediates was explored using assays previously developed to isolate distinct mechanisms of soluble A $\beta$  aggregate growth (Nichols et al., 2002). This molecule was found to effectively inhibit the lateral association of soluble A $\beta$ <sub>1-40</sub> aggregates (Figs. 5D-F and 6A), illustrating that compound **2** is capable of binding on-pathway intermediates to prevent their progression into larger structures. By evaluating reductions in the association rate, an IC<sub>50</sub> at a stoichiometric ratio of 0.92 inhibitor to monomeric units of A $\beta$ <sub>1-40</sub> was determined for inhibition of soluble aggregate association (Fig. 6B). This somewhat lower stoichiometry, relative to inhibition of HFIP-induced monomer aggregation,

may suggest that compound **2** is capable of binding both larger aggregation intermediates as well as aggregate structures that appear very early in the self-assembly pathway. These early aggregates would be absent from SEC-isolated soluble aggregate preparations that are derived from self-assembly reactions at relatively late time points. Alternatively, the difference in stoichiometry might reflect the morphological differences reported for aggregates formed in dilute HFIP versus aqueous buffer (Nichols et al., 2005).

In contrast to association, compound **2** was incapable of inhibiting elongation of soluble A $\beta_{1-40}$  aggregates via monomer addition (Figs. 4 and 5A-C). The negligible inhibition of monomer addition to aggregated protein is similar to that observed for methylene blue (Necula et al., 2007a), Congo Red (LeVine, 2007), and nordihydroguaiaretic acid (Moss et al., 2004). However, other small molecules have been shown to inhibit A $\beta$  fibril extension by monomer addition (Dolphin et al., 2008; Naiki et al., 1998; Ono et al., 2004; Ono et al., 2003; Williams et al., 2005). Because compound **2** does not reduce monomer available for addition to pre-formed aggregates, this result provides additional evidence that compound **2** does not bind monomeric A $\beta_{1-40}$ . Furthermore, the selectivity of compound **2** for inhibition of soluble A $\beta_{1-40}$  aggregate growth by lateral association demonstrates that binding of compound **2** to aggregated protein structures does not block sites of monomer addition. Instead, binding sites for this compound may be situated along the lateral surface of aggregates, positioning the bound inhibitor to selectively block association events. A similar selectivity was observed for the inhibition of soluble A $\beta_{1-40}$  aggregate growth by nordihydroguaiaretic acid (Moss et al., 2004).

As opposed to elongation in which monomers undergo a random coil to  $\beta$ -sheet transition upon incorporation into aggregate structures, association involves the coalescence of existing  $\beta$ -sheet structures and therefore does not create new amyloid material. Hence, selective

inhibition of aggregate association might not be expected to impact aggregate formation from monomeric protein. Here, however, inhibition was observed for both aggregate association and monomer aggregation, suggesting that the ability of intermediate aggregates to associate contributes to the extent of aggregate formation. Association may create new sites for monomer addition or may stabilize aggregates to facilitate further aggregate growth. Still, complete blockage of fibril formation will require inhibition of both mechanisms of aggregate growth such that effective therapeutic strategies should employ multifunctional structures or multiple compounds.

The inhibitory activity observed for compound **2** may be attributed to its aromatic structure and the reactive aldehyde group that can bind amino residues of the peptide. Several small molecules containing aromatic structures have been identified as inhibitors of A $\beta$  self-assembly (reviewed in Findeis, 2000; Hamaguchi et al., 2006; LeVine, 2007). Some of these compounds are proposed to recognize A $\beta$  via interactions with aromatic residues (Barnham et al., 2008; Cellamare et al., 2008; Dolphin et al., 2008; Porat et al., 2006). In fact, aromatic residues are commonly found at critical positions within amyloidogenic proteins and may thermodynamically favor  $\beta$ -sheet formation (Gazit, 2002). A $\beta$  contains four aromatic residues, including phenylalanine at residues 4, 19, and 20 and tyrosine at residue 10. F19 and F20 lie within the hydrophobic core of the protein, which is essential to amyloid formation (Hilbich et al., 1992).  $\pi$ -stacking of aromatic residues is hypothesized to contribute to amyloid self-assembly (Gazit, 2002), and  $\pi$ -stacking of phenylalanine residues has been observed for other amyloid forming proteins (Jack et al., 2006).  $\pi$ - $\pi$  interactions are also suggested to participate in the recognition of A $\beta$  by small molecules containing aromatic structures (Barnham et al., 2008; Cellamare et al., 2008; De Felice et al., 2004; Dolphin et al., 2008; Kanapathipillai et al., 2005;

Porat et al., 2006). Thus,  $\pi$ - $\pi$  interactions between compound **2** and A $\beta$  may disturb  $\pi$ -stacking between protein units within the  $\beta$ -structure, leading to disruption of A $\beta$  self-assembly. The inference that compound **2** binds an on-pathway assembly intermediate suggests that A $\beta$  monomers must reside in a  $\beta$ -sheet conformation for  $\pi$ - $\pi$  interactions between the small molecule and the protein to occur. One proposed model for A $\beta$  aggregate structure (Petkova et al., 2002) places F19 and F20 within the  $\beta$ -sheet structure of A $\beta$  aggregates. Furthermore, these residues are positioned to participate in interactions involved in the lateral association of aggregates, which were found in the current study to be selectively disrupted by compound **2**. Also positioned at this lateral association interface, the primary amine of K16 may interact with the aldehyde group to enhance binding. Alternatively, interaction between the aldehyde and K28 may disrupt its participation in a salt bridge with D23 that is suggested to stabilize a predicted  $\beta$ -turn. However, these reactions will be relatively slow at the experimental pH of 8.0.

The current study identifies a novel inhibitor of A $\beta_{1-40}$  self-assembly. Using assays that isolate two distinct mechanisms of soluble A $\beta_{1-40}$  aggregate growth, a julolidine aldehyde is shown to selectively inhibit the growth of soluble aggregates by lateral association, while having little effect on soluble aggregate elongation via monomer addition. Parallel inhibition of aggregate formation from monomeric protein implicates a role for lateral aggregate association in the overall extent of aggregate formation. Together, these results imply that this compound binds the lateral surface of a soluble on-pathway intermediate to prevent association with other aggregates required for continued assembly into mature fibrils. Furthermore, IC<sub>50</sub> values suggest that a range of aggregate sizes may be recognized by this compound. These findings demonstrate that the quantitative evaluation of inhibition at different mechanistic steps within the

A $\beta$  self-assembly process can provide insight into the mechanism of inhibitor action to facilitate optimization of effective inhibitor structures.

## References

- Alzheimer's Association (2008) 2008 Alzheimer's disease facts and figures. *Alzheimers Dement* **4**(2):110-133.
- Barnham KJ, Kenche VB, Ciccotosto GD, Smith DP, Tew DJ, Liu X, Perez K, Cranston GA, Johanssen TJ, Volitakis I, Bush AI, Masters CL, White AR, Smith JP, Cherny RA and Cappai R (2008) Platinum-based inhibitors of amyloid- $\beta$  as therapeutic agents for Alzheimer's disease. *Proc Natl Acad Sci USA* **105**(19):6813-6818.
- Bastianetto S, Yao ZX, Papadopoulos V and Quirion R (2006) Neuroprotective effects of green and black teas and their catechin gallate esters against  $\beta$ -amyloid-induced toxicity. *Eur J Neurosci* **23**(1):55-64.
- Bohrmann B, Adrian M, Dubochet J, Kuner P, Muller F, Huber W, Nordstedt C and Dobeli H (2000) Self-assembly of  $\beta$ -amyloid 42 is retarded by small molecular ligands at the stage of structural intermediates. *J Struct Biol* **130**(2-3):232-246.
- Byeon SR, Lee JH, Sohn JH, Kim DC, Shin KJ, Yoo KH, Mook-Jung I, Lee WK and Kim DJ (2007) Bis-styrylpyridine and bis-styrylbenzene derivatives as inhibitors for A $\beta$  fibril formation. *Bioorg Med Chem Lett* **17**(5):1466-1470.
- Cellamare S, Stefanachi A, Stolfa DA, Basile T, Catto M, Campagna F, Sotelo E, Acquafredda P and Carotti A (2008) Design, synthesis, and biological evaluation of glycine-based molecular tongs as inhibitors of A $\beta$ 1-40 aggregation *in vitro*. *Bioorg Med Chem* **16**(9):4810-4822.
- De Felice FG and Ferreira ST (2002)  $\beta$ -amyloid production, aggregation, and clearance as targets for therapy in Alzheimer's disease. *Cell Mol Neurobiol* **22**(5-6):545-563.

- De Felice FG, Vieira MN, Saraiva LM, Figueroa-Villar JD, Garcia-Abreu J, Liu R, Chang L, Klein WL and Ferreira ST (2004) Targeting the neurotoxic species in Alzheimer's disease: inhibitors of A $\beta$  oligomerization. *FASEB J* **18**(12):1366-1372.
- Dolphin GT, Chierici S, Ouberai M, Dumy P and Garcia J (2008) A multimeric quinacrine conjugate as a potential inhibitor of Alzheimer's  $\beta$ -amyloid fibril formation. *Chembiochem* **9**(6):952-963.
- Ferrao-Gonzales AD, Robbs BK, Moreau VH, Ferreira A, Juliano L, Valente AP, Almeida FC, Silva JL and Foguel D (2005) Controlling  $\beta$ -amyloid oligomerization by the use of naphthalene sulfonates: Trapping low molecular weight oligomeric species. *J Biol Chem* **280**(41):34747-34754.
- Findeis MA (2000) Approaches to discovery and characterization of inhibitors of amyloid  $\beta$ -peptide polymerization. *Biochem Biophys Acta* **1502**(1):76-84.
- Gazit E (2002) A possible role for  $\pi$ -stacking in the self-assembly of amyloid fibrils. *FASEB J* **16**(1):77-83.
- Gonzalez-Velasquez FJ and Moss MA (2008) Soluble aggregates of the amyloid- $\beta$  protein activate endothelial monolayers for adhesion and subsequent transmigration of monocyte cells. *J Neurochem* **104**(2):500-513.
- Guntert A, Dobeli H and Bohrmann B (2006) High sensitivity analysis of amyloid- $\beta$  peptide composition in amyloid deposits from human and PS2APP mouse brain. *Neuroscience* **143**(2):461-475.
- Hamaguchi T, Ono K and Yamada M (2006) Anti-amyloidogenic therapies: strategies for prevention and treatment of Alzheimer's disease. *Cell Mol Life Sci* **63**(13):1538-1552.

- Hilbich C, Kisters-Woike B, Reed J, Masters CL and Beyreuther K (1992) Substitutions of hydrophobic amino acids reduce the amyloidogenicity of Alzheimer's disease  $\beta$ A4 peptides. *J Mol Biol* **228**:460-473.
- Howlett DR, George AR, Owen DE, Ward RV and Markwell RE (1999a) Common structural features determine the effectiveness of carvedilol, daunomycin and rolitetracycline as inhibitors of Alzheimer  $\beta$ -amyloid fibril formation. *Biochem J* **343**(Pt 2):419-423.
- Howlett DR, Perry AE, Godfrey F, Swatton JE, Jennings KH, Spitzfaden C, Wadsworth H, Wood SJ and Markwell RE (1999b) Inhibition of fibril formation in  $\beta$ -amyloid peptide by a novel series of benzofurans. *Biochem J* **340**(Pt 1):283-289.
- Jack E, Newsome M, Stockley PG, Radford SE and Middleton DA (2006) The organization of aromatic side groups in an amyloid fibril probed by solid-state  $^2\text{H}$  and  $^{19}\text{F}$  NMR spectroscopy. *J Am Chem Soc* **128**(25):8098-8099.
- Kanapathipillai M, Lentzen G, Sierks M and Park CB (2005) Ectoine and hydroxyectoine inhibit aggregation and neurotoxicity of Alzheimer's  $\beta$ -amyloid. *FEBS Lett* **579**(21):4775-4780.
- Kirkitadze MD, Bitan G and Teplow DB (2002) Paradigm shifts in Alzheimer's disease and other neurodegenerative disorders: The emerging role of oligomeric assemblies. *J Neurosci Res* **69**(5):567-577.
- Kotarek JA, Johnson KC and Moss MA (2008) Quartz crystal microbalance analysis of growth kinetics for aggregation intermediates of the amyloid-beta protein. *Anal Biochem* **378**(1):15-24.
- Lashuel HA, Hartley DM, Balakhaneh D, Aggarwal A, Teichberg S and Callaway DJ (2002) New class of inhibitors of amyloid- $\beta$  fibril formation. Implications for the mechanism of pathogenesis in Alzheimer's disease. *J Biol Chem* **277**(45):42881-42890.

- LeVine H, 3rd (2005) Multiple ligand binding sites on A $\beta$ (1-40) fibrils. *Amyloid* **12**(1):5-14.
- LeVine H, 3rd (2007) Small molecule inhibitors of A $\beta$  assembly. *Amyloid* **14**(3):185-197.
- Moss MA, Varvel NH, Nichols MR, Reed DK and Rosenberry TL (2004) Nordihydroguaiaretic acid does not disaggregate  $\beta$ -amyloid(1-40) protofibrils but does inhibit growth arising from direct protofibril association. *Mol Pharmacol* **66**:592-600.
- Naiki H, Hasegawa K, Yamaguchi I, Nakamura H, Gejyo F and Nakakuki K (1998) Apolipoprotein E and antioxidants have different mechanisms of inhibiting Alzheimer's  $\beta$ -amyloid fibril formation *in vitro*. *Biochemistry* **37**:17882-17889.
- Necula M, Breydo L, Milton S, Kaye R, van der Veer WE, Tone P and Glabe CG (2007a) Methylene blue inhibits amyloid A $\beta$  oligomerization by promoting fibrillization. *Biochemistry* **46**(30):8850-8860.
- Necula M, Kaye R, Milton S and Glabe CG (2007b) Small molecule inhibitors of aggregation indicate that amyloid  $\beta$  oligomerization and fibrillization pathways are independent and distinct. *J Biol Chem* **282**(14):10311-10324.
- Nichols MR, Moss MA, Reed DK, Cratic-McDaniel S, Hoh JH and Rosenberry TL (2005) Amyloid- $\beta$  protofibrils differ from amyloid- $\beta$  aggregates induced in dilute hexafluoroisopropanol in stability and morphology. *J Biol Chem* **280**(4):2471-2480.
- Nichols MR, Moss MA, Reed DK, Lin W-L, Mukhopadhyay R, Hoh JH and Rosenberry TL (2002) Growth of  $\beta$ -amyloid(1-40) protofibrils by monomer elongation and lateral association. Characterization of distinct products by light scattering and atomic force microscopy. *Biochemistry* **41**(19):6115-6127.

- Ono K, Hasegawa K, Naiki H and Yamada M (2004) Anti-amyloidogenic activity of tannic acid and its activity to destabilize Alzheimer's  $\beta$ -amyloid fibrils *in vitro*. *Biochim Biophys Acta* **1690**(3):193-202.
- Ono K, Yoshiike Y, Takashima A, Hasegawa K, Naiki H and Yamada M (2003) Potent anti-amyloidogenic and fibril-destabilizing effects of polyphenols *in vitro*: implications for the prevention and therapeutics of Alzheimer's disease. *J Neurochem* **87**(1):172-181.
- Petkova AT, Ishii Y, Balbach JJ, Antzutkin ON, Leapman RD, Delaglio F and Tycko R (2002) A structural model for Alzheimer's  $\beta$ -amyloid fibrils based on experimental constraints from solid state NMR. *Proc Natl Acad Sci USA* **99**(26):16742-16747.
- Porat Y, Abramowitz A and Gazit E (2006) Inhibition of amyloid fibril formation by polyphenols: structural similarity and aromatic interactions as a common inhibition mechanism. *Chem Biol Drug Des* **67**(1):27-37.
- Reinke AA and Gestwicki JE (2007) Structure-activity relationships of amyloid  $\beta$ -aggregation inhibitors based on curcumin: influence of linker length and flexibility. *Chem Biol Drug Des* **70**(3):206-215.
- Simons LJ, Caprathe BW, Callahan M, Graham JM, Kimura T, Lai Y, Levine H, 3rd, Lipinski W, Sakkab AT, Tasaki Y, Walker LC, Yasunaga T, Ye Y, Zhuang N and Augelli-Szafran CE (2009) The synthesis and structure-activity relationship of substituted N-phenyl anthranilic acid analogs as amyloid aggregation inhibitors. *Bioorg Med Chem Lett* **19**(3):654-657.
- Walsh DM and Selkoe DJ (2007) A $\beta$  oligomers - A decade of discovery. *J Neurochem* **101**(5):1172-1184.

Williams AD, Segal M, Chen M, Kheterpal I, Geva M, Berthelier V, Kaleta DT, Cook KD and Wetzel R (2005) Structural properties of A $\beta$  protofibrils stabilized by a small molecule. *Proc Natl Acad Sci USA* **102**(20):7115-7120.

Yang F, Lim GP, Begum AN, Ubada OJ, Simmons MR, Ambegaokar SS, Chen PP, Kaye R, Glabe CG, Frautschy SA and Cole GM (2005) Curcumin inhibits formation of amyloid  $\beta$  oligomers and fibrils, binds plaques, and reduces amyloid *in vivo*. *J Biol Chem* **280**(7):5892-5901.

## Footnotes

The authors would like to acknowledge the University of South Carolina Electron Microscopy Center for instrument use as well as scientific and technical assistance. This work was supported by a grant from the National Science Foundation Early Career Development Program (CAREER) [CBET-0644826]. Any opinions, findings, and conclusions or recommendations expressed in this material are those of the authors and do not necessarily reflect the views of the National Science Foundation. In addition, this work was supported by a Graduate Fellowship from the Alfred P. Sloan Foundation Minority Ph.D. Program, a Graduate Fellowship from the South East Alliance for Graduate Education and the Professoriate (SEAGEP), and a Graduate Research Fellowship from the University of South Carolina College of Arts and Sciences.

Please address requests for reprints to: Melissa A. Moss, Department of Chemical Engineering, University of South Carolina, 301 Main Street, Columbia, SC 29208; email: [mossme@cec.sc.edu](mailto:mossme@cec.sc.edu).

<sup>1</sup>Current Address: Eastman Chemical Company, B-66 CE Technology, Kingsport, TN 37662.

## Figure Legends

### Scheme 1 Synthesis of compound 2.

**Fig. 1** Effect of compound **2** on A $\beta_{1-40}$  monomer aggregation. A $\beta_{1-40}$  monomer diluted to 20  $\mu$ M in buffer containing 150 mM NaCl and 40 mM Tris-HCl (pH 8.0) was incubated alone (control,  $\circ$ ) or in the presence of 20  $\mu$ M ( $\blacktriangle$ ), 40  $\mu$ M ( $\blacktriangle$ ), or 400  $\mu$ M ( $\blacktriangle$ ) compound **2**. All reactions additionally contained 2.5% DMSO to facilitate solubilization of compound **2**. Aggregation of monomer was induced by continuous agitation and monitored via ThT fluorescence (F) by periodic dilution into 10  $\mu$ M ThT. Results are representative of three independent experiments.

**Fig. 2** ThT detection of pre-formed A $\beta_{1-40}$  aggregates in the presence of compound **2**. A $\beta_{1-40}$  aggregates formed in the absence of compound **2** were diluted to 2  $\mu$ M ( $\blacktriangle$ ) or 20  $\mu$ M ( $\blacktriangledown$ ) in 40 mM Tris-HCl (pH 8.0) containing 10  $\mu$ M ThT or 40  $\mu$ M ThT, respectively, and incubated alone (0  $\mu$ M, control) or in the presence of concentrations of compound **2** ranging from 3  $\mu$ M to 500  $\mu$ M. All incubations additionally contained 2.5% DMSO to facilitate solubilization of compound **2**. Aggregates were detected using ThT fluorescence, and the percentage of ThT fluorescence detection was determined relative to control samples. Points at 0  $\mu$ M inhibitor were performed with 2 repetitions; points at 30  $\mu$ M inhibitor were performed with 3 repetitions; points at 60  $\mu$ M inhibitor were performed with 4 repetitions. Error bars represent SEM. Error bars lie within symbols.

**Fig. 3** Effect of compound **2** on HFIP-induced  $A\beta_{1-40}$  monomer aggregation. (A)  $A\beta_{1-40}$  monomer in 40 mM Tris-HCl (pH 8.0) was pre-incubated for 15 min alone or in the presence of compound **2**. Solutions were then diluted for final concentrations of compound **2** ranging from 60  $\mu$ M to 200  $\mu$ M with 20  $\mu$ M  $A\beta_{1-40}$  monomer, and 2.5% HFIP was added to induce aggregate formation in the absence of agitation. All reactions additionally contained 2.5% DMSO to facilitate solubilization of compound **2**. Aggregate formation was continuously monitored *in situ* via ThT fluorescence (F) by the inclusion of 40  $\mu$ M ThT in the reaction mixture. (B) HFIP-induced aggregation of 20  $\mu$ M  $A\beta_{1-40}$  monomer was measured as in panel A for monomer incubated alone (0  $\mu$ M, control) or with concentrations of compound **2** ranging from 20  $\mu$ M to 500  $\mu$ M, giving ratios of compound **2** to  $A\beta_{1-40}$  monomer ranging from 1 to 25. Aggregate formation was determined from the plateau ThT fluorescence and is expressed as a percentage of the positive control. An  $IC_{50}$  value of 6.8 was derived from nonlinear regression of the data ( $r^2 = 0.99$ ) by fixing the maximum and minimum values at 100% and 0%, respectively, and allowing the Hill slope to vary. Results are representative of two independent experiments.

**Fig. 4** Effect of compound **2** on soluble  $A\beta_{1-40}$  aggregate growth via monomer addition. SEC-isolated soluble  $A\beta_{1-40}$  aggregates in 40 mM Tris-HCl (pH 8.0) were pre-incubated for 15 min alone or in the presence of compound **2**. Solutions were then diluted for final concentrations of 1  $\mu$ M soluble  $A\beta_{1-40}$  aggregates with 0  $\mu$ M (positive control,  $\circ$ ), 1  $\mu$ M ( $\blacktriangle$ ), 5  $\mu$ M ( $\blacktriangledown$ ), 30  $\mu$ M ( $\blacktriangle$ ), or 80  $\mu$ M ( $\blacktriangledown$ ) compound **2**, and 20  $\mu$ M  $A\beta_{1-40}$  monomer was added to induce aggregate growth. As negative controls, 1  $\mu$ M soluble  $A\beta_{1-40}$  aggregates ( $\square$ ) or 20  $\mu$ M  $A\beta_{1-40}$  monomer ( $\diamond$ ) were incubated alone. All reactions additionally contained 2.5% DMSO to facilitate solubilization of compound **2**. Incorporation of  $A\beta_{1-40}$  monomer into fibrillar structures

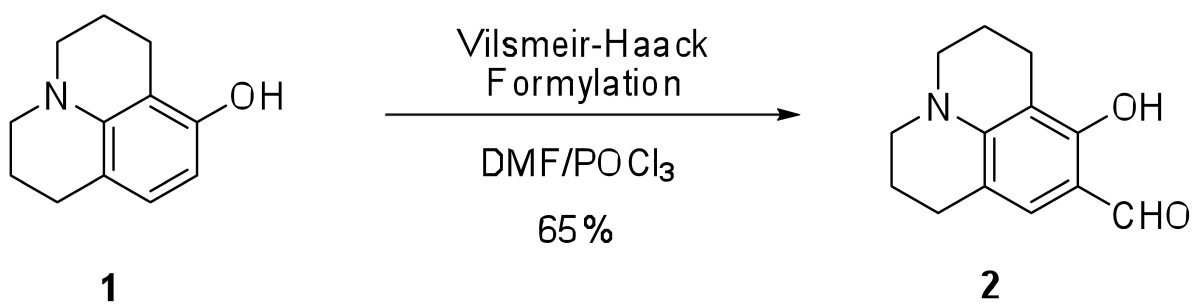
was monitored *in situ* as the change in ThT fluorescence ( $\Delta F$ ) by the inclusion of 10  $\mu\text{M}$  ThT in the reaction mixture. Results are representative of three independent experiments.

**Fig. 5** Morphology of  $\text{A}\beta_{1-40}$  aggregates. 2  $\mu\text{M}$  SEC-isolated soluble  $\text{A}\beta_{1-40}$  aggregates in 40 mM Tris-HCl (pH 8.0) were incubated alone (panels A and D, negative control), elongated in the presence of 20  $\mu\text{M}$   $\text{A}\beta_{1-40}$  monomer (panel B, positive control), elongated in the presence of 20  $\mu\text{M}$   $\text{A}\beta_{1-40}$  monomer and 60  $\mu\text{M}$  compound **2** (panel C), associated in the presence of 150 mM NaCl (panel E, positive control), or associated in the presence of 150 mM NaCl and 40  $\mu\text{M}$  compound **2** (panel F). For samples containing compound **2**, soluble aggregates and compound **2** were pre-incubated for 15 min prior to initiation of aggregate growth. Following 30 min of aggregate growth, samples were gridded and visualized by TEM as described under Materials and Methods. Results are representative of two independent experiments. Images are shown relative to a scale bar of 0.5  $\mu\text{m}$ .

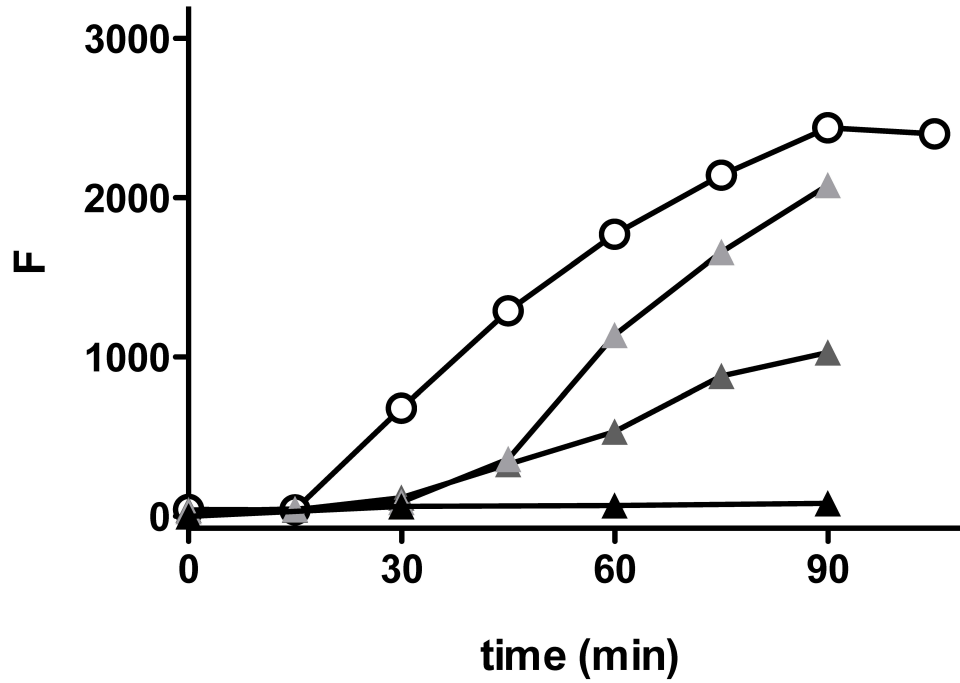
**Fig. 6** Effect of compound **2** on soluble  $\text{A}\beta_{1-40}$  aggregate growth via association. (A) SEC-isolated soluble  $\text{A}\beta_{1-40}$  aggregates in 40 mM Tris-HCl (pH 8.0) were pre-incubated for 15 min alone or in the presence of compound **2**. Solutions were then diluted for final concentrations of 2  $\mu\text{M}$  soluble  $\text{A}\beta_{1-40}$  aggregates with 0  $\mu\text{M}$  (positive control,  $\circ$ ), 2  $\mu\text{M}$  ( $\blacktriangle$ ), or 4.3  $\mu\text{M}$  ( $\blacktriangle$ ) compound **2**, and 260 mM NaCl was added to induce aggregate association. As a negative control, 2  $\mu\text{M}$  soluble  $\text{A}\beta_{1-40}$  aggregates ( $\square$ ) were incubated alone and in the absence of NaCl. All reactions additionally contained 2.5% DMSO to facilitate solubilization of compound **2**. Increases in aggregate size were continuously monitored as changes in  $R_H$  using DLS. Linear regression (solid lines) was performed to determine association growth rates ( $r^2 \geq 0.85$ ). Results

are representative of three independent experiments. (B) Association of 1  $\mu\text{M}$  ( $\blacktriangle$ ) or 2  $\mu\text{M}$  ( $\blacktriangledown$ ) SEC-isolated soluble  $\text{A}\beta_{1-40}$  aggregates was stimulated by the presence of 150-300 mM NaCl for soluble aggregates incubated alone (0  $\mu\text{M}$ , control) or with concentrations of compound **2** ranging from 0.1  $\mu\text{M}$  to 40  $\mu\text{M}$ , giving ratios of compound **2** to  $\text{A}\beta_{1-40}$  aggregate ranging from 0.1 to 20. Association rates were calculated as in panel A and are expressed as a percentage of positive control. An  $\text{IC}_{50}$  value of 0.92 was derived from nonlinear regression of the data ( $r^2 = 0.99$ ) by fixing the maximum and minimum values at 100% and 10%, respectively, and allowing the Hill slope to vary. Data shown is from five independent experiments.

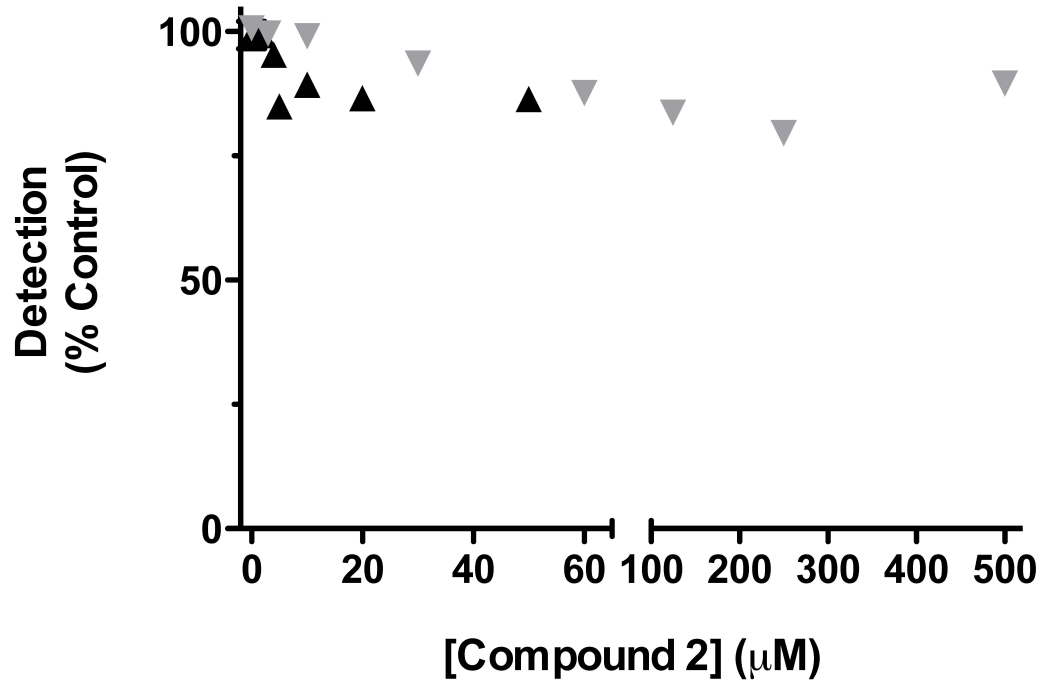
**MOL #55301**  
**Scheme 1**

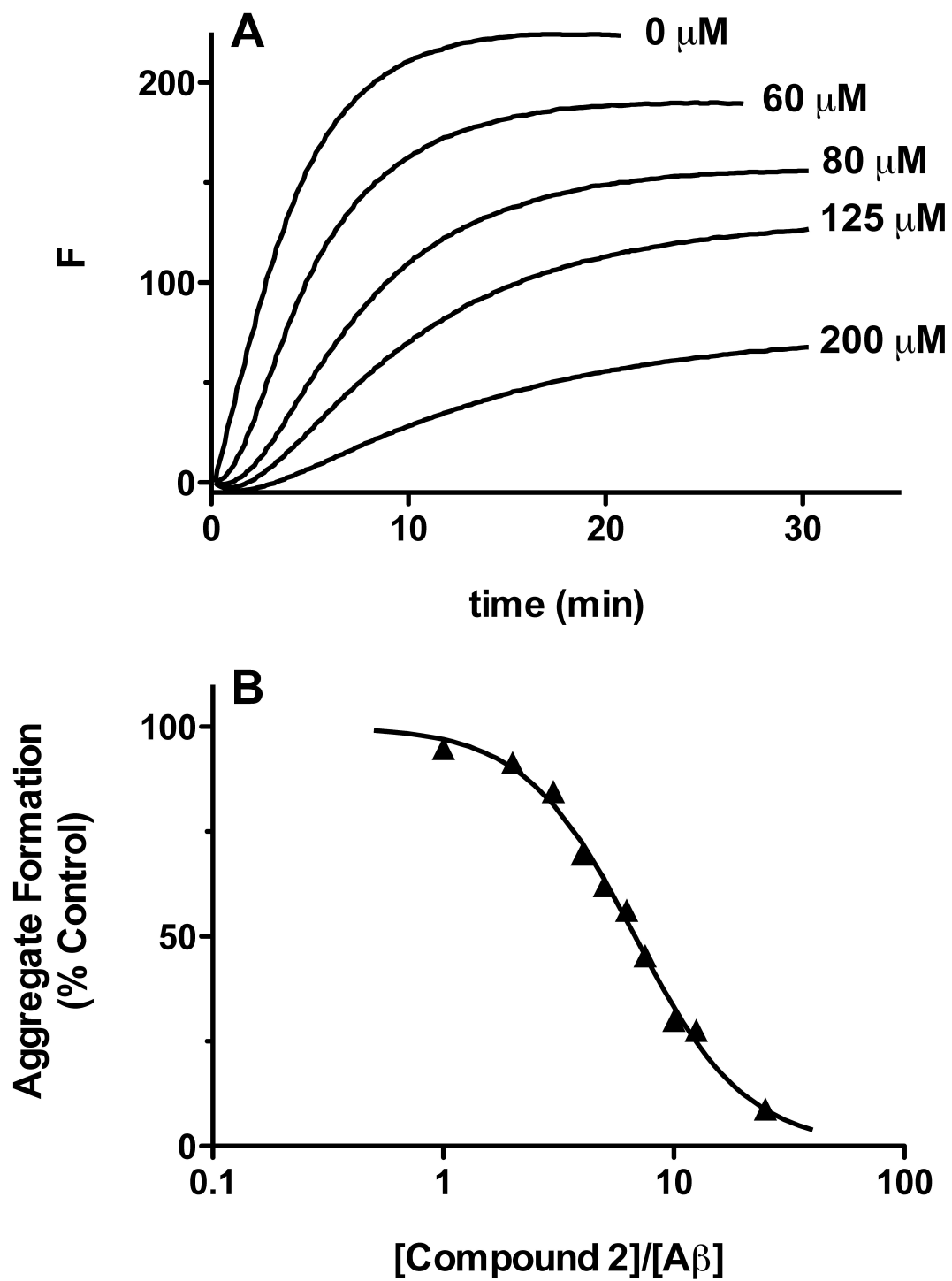


**MOL #55301**  
**Fig. 1**

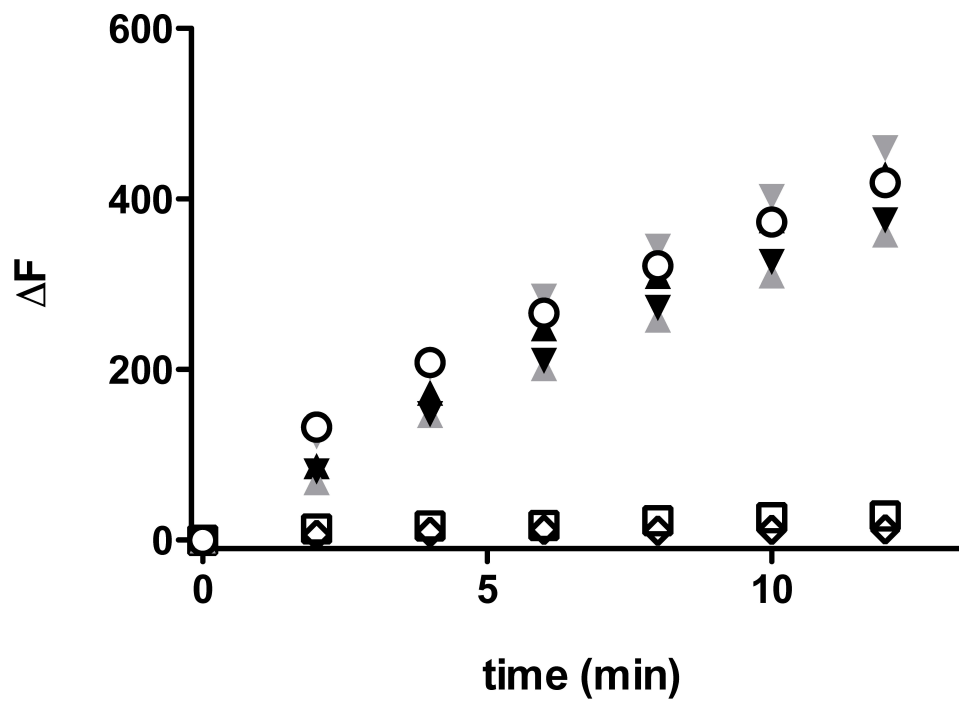


**MOL #55301**  
**Fig. 2**





**MOL #55301**  
**Fig. 4**



**MOL #55301**  
**Fig. 5**

